IL NUOVO CIMENTO **44 C** (2021) 87
DOI 10.1393/ncc/i2021-21087-4

Communications: SIF Congress 2020

Clusters morphology by Zernike polynomials

V. Capalbo(1), M. De Petris(1), F. De Luca(1)(2), W. Cui(3), G. Yepes(4)(5), A. Knebe(4)(5)(6) and E. Rasia(7)(8)

(1) *Dipartimento di Fisica, Sapienza Università di Roma - Roma, Italy*
(2) *Dipartimento di Fisica, Università di Roma "Tor Vergata" - Roma, Italy*
(3) *Institute for Astronomy, University of Edinburgh, Royal Observatory - Edinburgh, UK*
(4) *Departamento de Física Teórica, Universidad Autónoma de Madrid - Madrid, Spain*
(5) *CIAFF, Universidad Autónoma de Madrid - Madrid, Spain*
(6) *ICRAR, University of Western Australia - Crawley, Western Australia, Australia*
(7) *INAF, Osservatorio Astronomico di Trieste - Trieste, Italy*
(8) *Institute for Fundamental Physics of the Universe (IFPU) - Trieste, Italy*

received 15 January 2021

Summary. — The study of the morphology of multiwavelength images of galaxy clusters is largely used to infer their dynamical state. We presented a novel approach of morphological analysis based on modelling clusters images with Zernike polynomials (ZPs). We used mock maps of the thermal component of the Sunyaev-Zel'dovich (tSZ) effect generated for synthetic clusters in THE THREE HUNDRED project, in the redshift range $0 \leq z \leq 1.03$. Each tSZ map was modelled with several ZPs, in order to recover morphological features that could be related to different dynamical states. We concluded that morphological differences can be quantified by defining an indicator that includes the contribution of the different ZPs to the fit of the tSZ maps. The feasibility of this new method is prone to the angular resolution of the maps. Our results were also correlated with common morphological parameters and dynamical state indicators applied on the same clusters sample.

1. – Introduction

Galaxy clusters can be used as cosmological probes since their abundance in the Universe, *i.e.*, the number of clusters of a given mass per Mpc^3, and its evolution with redshift are sensitive to some parameters defining the cosmological model [1]. We need to correctly estimate the total mass of the clusters, even if it is not a direct observable and must be inferred by exploiting other quantities that trace its value, at different wavelengths. In particular, a few simplified assumptions about the physics of the clusters, such as the hydrostatic and thermal balance, are generally used to define some observables-mass relations [2]. However, these conditions not always reflect the real state of the clusters, which could be in dynamical states far from the equilibrium. Hence, the knowledge of the dynamical state assumes an important role when studying these objects.

The morphological analysis of multiwavelenght images is commonly used as indication of the clusters real state. It consists in applying some parameters to recognize characteristic features in the distribution of the signal, even if with some limitations due, for example, to projection effects along the line of sight and limited observational angular resolutions. Simulation-based analysis are also used to test and direct the correct application of the different parameters on the observational data.

Here we summarize the results of a work originally presented in [3], which focused on the development of a new method of morphological analysis of clusters images by means of Zernike polynomials (ZPs) [4]. We used a set of synthetic galaxy clusters extracted from hydrodynamical simulations, THE THREE HUNDRED project [5], including 324 massive clusters ($M_{200} > 6 \times 10^{14}\ h^{-1}\mathrm{M}_{\odot}$ at $z = 0$) at different redshifts from 0 up to 1.03. To study the clusters we exploited the thermal component of the Sunyaev-Zel'dovich (tSZ) effect [6], that is a spectral distortion of the Cosmic Microwave Background due to inverse Compton scattering between photons and energetic free electrons in the hot ionized plasma within the clusters. It is quantified with the Compton parameter y:

$$y(\hat{n}) = \frac{\sigma_T k_B}{m_e c^2} \int P_e(\hat{n}, l)\mathrm{d}l, \tag{1}$$

where σ_T is the Thomson scattering cross-section, k_B is the Boltzmann constant, m_e is the electron mass, c is the speed of light and P_e is the electron pressure integrated along the line of sight l in the direction $\hat{n}$. Mock tSZ maps, that are 2D projections of the Compton parameter, *i.e.*, y-maps, were generated for all the clusters with the PyMSZ code(1). We analytically modelled them with several ZPs, within a circular aperture of radius equal to R_{500}(2), the clusters reference radius, and centred on the y-centroid. We also applied a smoothing to degrade the signal in the maps and mimic observational angular resolutions up to $5'$.

2. – Zernike polynomials: definition and application

Zernike polynomials are a complete and orthogonal basis of polynomials defined on a unit circle, useful to model functions in a circular domain. They have several applications in different fields: adaptive optics [7, 8], image analysis and pattern recognition [9], ophthalmology and optometry [10], medicine [11]. The work in [3] is their first application in the galaxy clusters science.

We referred to [7] for the mathematical definition of the ZPs, which result in a product of a normalization factor N, a radial function R and an angular term:

$$\begin{cases} Z_n^m(\rho, \theta) = N_n^m R_n^m(\rho)\cos(m\theta), \\ Z_n^{-m}(\rho, \theta) = N_n^m R_n^m(\rho)\sin(m\theta), \end{cases} \tag{2}$$

where $N_n^m = \sqrt{\frac{2(n+1)}{1+\delta_{m0}}}$ and $R_n^m(\rho) = \sum_{s=0}^{(n-m)/2} \frac{(-1)^s(n-s)!}{s!\left(\frac{n+m}{2}-s\right)!\left(\frac{n-m}{2}-s\right)!}\,\rho^{n-2s}$. The polar coordinates ρ and θ are the normalised radial distance ($0 \le \rho \le 1$) and the azimuthal

(1) `https://github.com/weiguangcui/pymsz`
(2) R_{500} is the radius within which the overdensity of the cluster is 500 times the critical density of the Universe at the cluster redshift.

angle ($0 \leq \theta \leq 2\pi$), respectively, while the index n is the polynomial order and the index m is the angular frequency, satisfying $m \leq n$ and $n - m =$ even.

We decomposed each y-map using all ZPs up to the eighth order, namely 45 polynomials (see the ordering sequence defined in [7]), in order to be able to model the different shapes of the signal at different spatial scales in the maps. For this purpose, we divided the set of ZPs in two classes, considering their 2D projections: polynomials with a continuous circular symmetry, that are all terms with $m = 0$, and polynomials with more complex patterns due to increasing angular frequency, *i.e.*, all terms with $m \neq 0$. Hence, the y-maps were expressed as a weighted sum given by

$$y = \sum_{n=0}^{8} \sum_{m=0}^{n} c_{nm} Z_n^m, \tag{3}$$

where the coefficients c_{nm} are the weights (Zernike coefficients) of the single polynomials.

3. – Results

To show how the Zernike fitting can be used to extract information about the morphology and the state of a cluster, we plot in fig. 1 a bar chart of the resulting coefficients c_{nm} from the fit of two y-maps. These relate to two clusters at $z = 0$, namely the #153 (in grey) and #171 (in white) in the catalogue, classified respectively as relaxed and disturbed objects in a previous analysis in [12]. We recall that "relaxed" and "disturbed" terms are generally used to identify, respectively, clusters in hydrostatic equilibrium and dynamically active systems far from this condition (*e.g.*, clusters in merging processes). The filled bars in fig. 1 refer to ZPs with $m \neq 0$, while the hatched bars refer to terms with $m = 0$. Note that the first polynomial, $Z_0^0 = 1$, is neglected because the respective coefficient c_{00} is simply equal to the mean value of y over the circular aperture. In addition, to better display the figure, we only show few terms of the fitting. However,

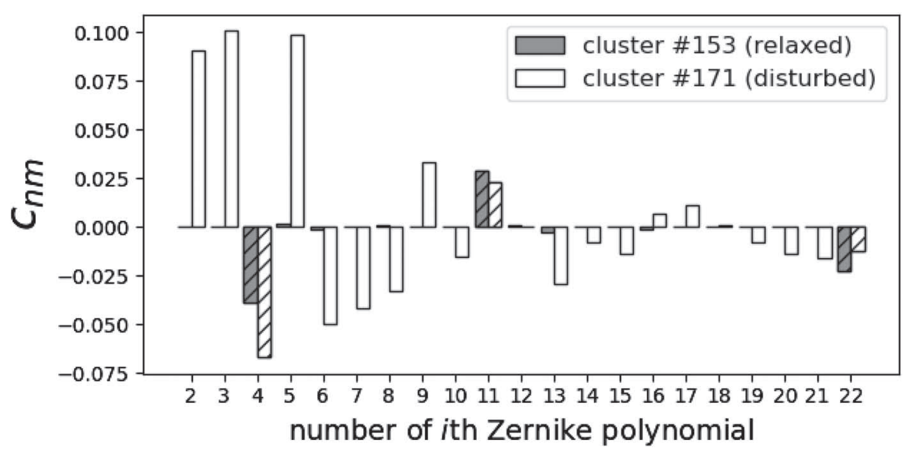

Fig. 1. – Bar chart of coefficients c_{nm}, resulting from a Zernike fitting applied to y-maps (see eq. (3)) of a relaxed cluster (in grey) and a disturbed one (in white). The Zernike polynomials, on the x-axis, are ordered as in [7]. The filled and hatched bars refer, respectively, to polynomials with $m \neq 0$ and $m = 0$ (see eq. (2)).

the considerations below are referred to the whole set of ZPs used. We note that the contribution of ZPs with $m \neq 0$ is negligible for the relaxed cluster, while ZPs with $m = 0$ are present in both cases. In general, maps of relaxed clusters show regular shapes, mostly circular, that can be modelled by few ZPs with circular symmetry, *i.e.*, $m = 0$. On the contrary, maps of disturbed clusters involve inhomogeneities and small-scale structures, and require additional polynomials to be correctly described. To quantify the differences between regular and irregular morphologies, we defined a parameter, $\mathcal{C}$, as follows [3]:

$$\mathcal{C} = \sum_{n,m\neq 0} |c_{nm}|^{1/2}. \tag{4}$$

We compared the results of the Zernike fitting with a previous analysis made on the same data set in [12], using as references: i) a combined morphological parameter [13,14]; ii) a combined 3D dynamical-state indicator, available for hydrosimulated objects [12,15]. By analysing the whole clusters sample, we obtained a correlation about 78 per cent between $\mathcal{C}$ and the combined morphological parameter, fairly stable at the redshifts considered, while the correlation with the combined 3D indicator is about 62 per cent at $z = 0$ and slightly decreasing with the redshift. In addition, we verified that this method can be efficiently applied to maps generated with subarcminute angular resolutions when moving to high-redshift clusters ($z \simeq 1$).

4. – Conclusions

We used a new approach to study the morphology of galaxy clusters, that is an analytical modelling of 2D projections maps with the Zernike polynomials. The first application was on mock maps of the thermal component of the Sunyaev-Zel'dovich effect, generated for a sample of hydrosimulated clusters. By estimating the contribution of several polynomials in modelling the clusters maps, we verified that it is possible to recognize their characteristic shapes, and to correlate the results with more common morphological and dynamical-state indicators.

* * *

The authors acknowledge THE THREE HUNDRED Collaboration for the support.

REFERENCES

[1] Planck Collaboration VI, *Astron. Astrophys.*, **641** (2020) A6.
[2] Kravtsov A. V. and Borgani S., *Annu. Rev. Astron. Astrophys.*, **50** (2012) 353.
[3] Capalbo V. *et al.*, *Mon. Not. R. Astron. Soc.*, **503** (2021) 6155.
[4] Zernike F., *Mon. Not. R. Astron. Soc.*, **94** (1934) 377.
[5] Cui W. *et al.*, *Mon. Not. R. Astron. Soc.*, **480** (2018) 2898.
[6] Sunyaev R. A. and Zel'dovich Y. B., *Comments Astrophys. Space Phys.*, **4** (1972) 173.
[7] Noll R. J., *J. Opt. Soc. Am.*, **66** (1976) 207.
[8] Rigaut F. *et al.*, *Astron. Astrophys.*, **250** (1991) 280.
[9] Teague M. R, *J. Opt. Soc. Am.*, **70** (1980) 920.
[10] Liang J. and Williams D. R., *J. Opt. Soc. Am. A*, **14** (1997) 2873.
[11] Tahmasbi A., Saki F., Shokouhi S. B., *Comput. Biol. Med.*, **41** (2011) 726.
[12] De Luca F. *et al.*, preprint, arXiv:2011.09002.
[13] Rasia E., Meneghetti M., Ettori S., *Astron. Rev.*, **8** (2013) 40.
[14] Cialone G. *et al.*, *Mon. Not. R. Astron. Soc.*, **477** (2018) 139.
[15] Haggar R. *et al.*, *Mon. Not. R. Astron. Soc.*, **492** (2020) 6074.